

Geometric bonding effects in the X^2A_1 , $A^2\Sigma^+u$, and $B^2\Pi_{lg}$ states of Li_2F

Wright, K., Rogers, D., & Lane, I. (2009). Geometric bonding effects in the X^2A_1 , $A^2\Sigma^+$, and $B^2\Pi_g$ states of Li_2F . *Journal of Chemical Physics*, 131(10), [104306]. <https://doi.org/10.1063/1.3216378>

Published in:
Journal of Chemical Physics

Document Version:
Publisher's PDF, also known as Version of record

Queen's University Belfast - Research Portal:
[Link to publication record in Queen's University Belfast Research Portal](#)

Publisher rights
© 2009 The American Physical Society

General rights
Copyright for the publications made accessible via the Queen's University Belfast Research Portal is retained by the author(s) and / or other copyright owners and it is a condition of accessing these publications that users recognise and abide by the legal requirements associated with these rights.

Take down policy
The Research Portal is Queen's institutional repository that provides access to Queen's research output. Every effort has been made to ensure that content in the Research Portal does not infringe any person's rights, or applicable UK laws. If you discover content in the Research Portal that you believe breaches copyright or violates any law, please contact openaccess@qub.ac.uk.

Geometric bonding effects in the X²A₁, A²Σ⁺_u, and B²Π_g states of Li₂F

Kris W. A. Wright, Daniel E. Rogers, and Ian C. Lane

Citation: J. Chem. Phys. **131**, 104306 (2009); doi: 10.1063/1.3216373

View online: <http://dx.doi.org/10.1063/1.3216373>

View Table of Contents: <http://jcp.aip.org/resource/1/JCPSA6/v131/i10>

Published by the American Institute of Physics.

Additional information on J. Chem. Phys.

Journal Homepage: <http://jcp.aip.org/>

Journal Information: http://jcp.aip.org/about/about_the_journal

Top downloads: http://jcp.aip.org/features/most_downloaded

Information for Authors: <http://jcp.aip.org/authors>

ADVERTISEMENT

Instruments for advanced science

Gas Analysis



- dynamic measurement of reaction gas streams
- catalysis and thermal analysis
- molecular beam studies
- dissolved species probes
- fermentation, environmental and ecological studies

Surface Science



- UHV TPD
- SIMS
- end point detection in ion beam etch
- elemental imaging - surface mapping

Plasma Diagnostics



- plasma source characterization
- etch and deposition process
- reaction kinetic studies
- analysis of neutral and radical species

Vacuum Analysis



- partial pressure measurement and control of process gases
- reactive sputter process control
- vacuum diagnostics
- vacuum coating process monitoring

contact Hiden Analytical for further details

HIDEN
ANALYTICAL

info@hideninc.com
www.HidenAnalytical.com

CLICK to view our product catalogue



Geometric bonding effects in the X^2A_1 , $A^2\Sigma_u^+$, and $B^2\Pi_g$ states of Li_2F

Kris W. A. Wright, Daniel E. Rogers, and Ian C. Lane^{a)}Innovative Molecular Materials Group, School of Chemistry and Chemical Engineering,
Queen's University of Belfast, Stranmillis Road, Belfast BT9 5AG, United Kingdom

(Received 11 June 2009; accepted 11 August 2009; published online 11 September 2009)

Published *ab initio* and pseudopotential calculations for the dialkali halide systems suggest that the preferred colinear geometry is for the metal to approach the metal end of the alkali halide. Here, *ab initio* calculations on the Li_2F system reveal that the well depth on the halide side in this radical is much deeper and is a local saddle point associated with the ionic nonlinear global minima. Although many features of the pseudopotential surfaces are confirmed, significant differences are apparent including the existence of a linear excited $A^2\Sigma_u^+$ state instead of a triangular one, a considerably deeper global minimum some 50% lower in energy and a close approach between the X^2A_1 and the $A^2\Sigma_u^+$ states, with the $A^2\Sigma_u^+$ minimum 87 kJ mol^{-1} below the ground state asymptote. All the results can be rationalised as the avoided crossings between a long range, covalent potential dominant within the LiLiF geometry and an ionic state that forms the global minimum. Calculations on the third $^2A'$ potential indicate that even for $\text{Li}+\text{LiF}$ collisions at ultracold temperatures the collision dynamics could involve as many as three electronic states. © 2009 American Institute of Physics. [doi:10.1063/1.3216373]

I. INTRODUCTION

Recently in this journal, Koput¹ has published a high-level calculation of the lowest rovibrational levels of the Li_2F molecule based on coupled cluster singlet doublet (triplet) [CCSD(T)] *ab initio* points. In this paper, the lowest electronic states of Li_2F are investigated further and in particular attention is drawn to a second local minimum on the ground surface. The initial motive for looking at this radical was to calculate a high-level *ab initio* potential for the study of ultracold collisions between a lithium atom and LiF , the simplest example of a class of alkali-alkali halide systems that have not been investigated by modern quantum scattering techniques.

The pseudopotential treatment by Roach and Child² for the analogous $\text{K}+\text{NaCl}$ system suggests that the KNaCl linear geometry has a very shallow well, whereas KClNa exists as a saddle point on the ground state, but stabilized relative to the $\text{K}+\text{NaCl}$ asymptote. These two linear geometries are both around -25 kJ mol^{-1} relative to the reagents. The later study by Struve³ however suggests that the $MM'X$ geometry is the most stable and is deepest for the LiNaCl and Na_2Cl systems, while predicting there is no well for the MXM' geometry in Na_2Cl . In all the pseudopotential work, the global minimum was an equilateral triangle. Contemporaneous *ab initio* work by Pearson *et al.*⁴ on the Li_2F radical confirmed the presence of a linear potential well, though considerably shallower than the pseudopotential method. Only the LiLiF linear configuration was considered in that work so no comparison of the two linear geometries can be made.

The calculated triangular global minimum is confirmed by all subsequent *ab initio* treatments including Rehm *et al.*,⁵

Sengupta and Chandra,⁶ Veličković *et al.*⁷ and most recently Koput. The more recent work on the system has focused on the deep well present on the surface or on the calculation of the thermodynamic limits and has been inspired in part by the experimental verification of a stable Li_2F molecule by Polce and Wesdemiotis⁸ (after an earlier tentative claim had been made by Veljković *et al.*⁹) and its confirmation^{10,11} by Yokoyama *et al.* in 2000. These theoretical studies have used primarily single-reference *ab initio* techniques such as CCSD(T). Interestingly, Haketa *et al.*¹² has identified the $D_{\infty h}$ isomer as being deeper in energy than the corresponding $C_{\infty v}$ geometry, at odds with the Struve pseudopotential calculations, though this geometry is again unstable with respect to bending motion. The high-quality *ab initio* calculations of the surface here will clarify the shape of the lowest potential energy surface.

Pearson *et al.* also suggested that there would be no low lying excited state, a result in contradiction to the simple pseudopotential model. Gutowski and Simons¹³ investigated the lowest electronic states of both the neutral and anion and identified the presence of a number of excited states. The thesis work of Balint-Kurti¹⁴ presented an orthogonalised Moffitt (OM) calculation of the lowest electronic states of Li_2F , in both linear and C_{2v} geometries. The OM method corrects for the poor calculation of electron affinity common in early *ab initio* techniques. The most comprehensive *ab initio* work on the alkali-alkali halide system is an early configuration interaction (CI) study by Yamashita and Morokuma¹⁵ who studied the lowest four $^2A'$ and two $^2A''$ surfaces of $\text{K}+\text{NaCl}$ using an aug-cc-pVTZ equivalent basis set. They identify the predominant configuration of the ground state as the complex K^++NaCl^- and they suggest that as the K atom approaches the NaCl molecule it experiences a repulsive interaction until an electron transfer event takes place to form the ionic complex. This repulsive interaction

^{a)}Author to whom correspondence should be addressed. Telephone: +44-2890-97-4458. Electronic mail: i.lane@qub.ac.uk.

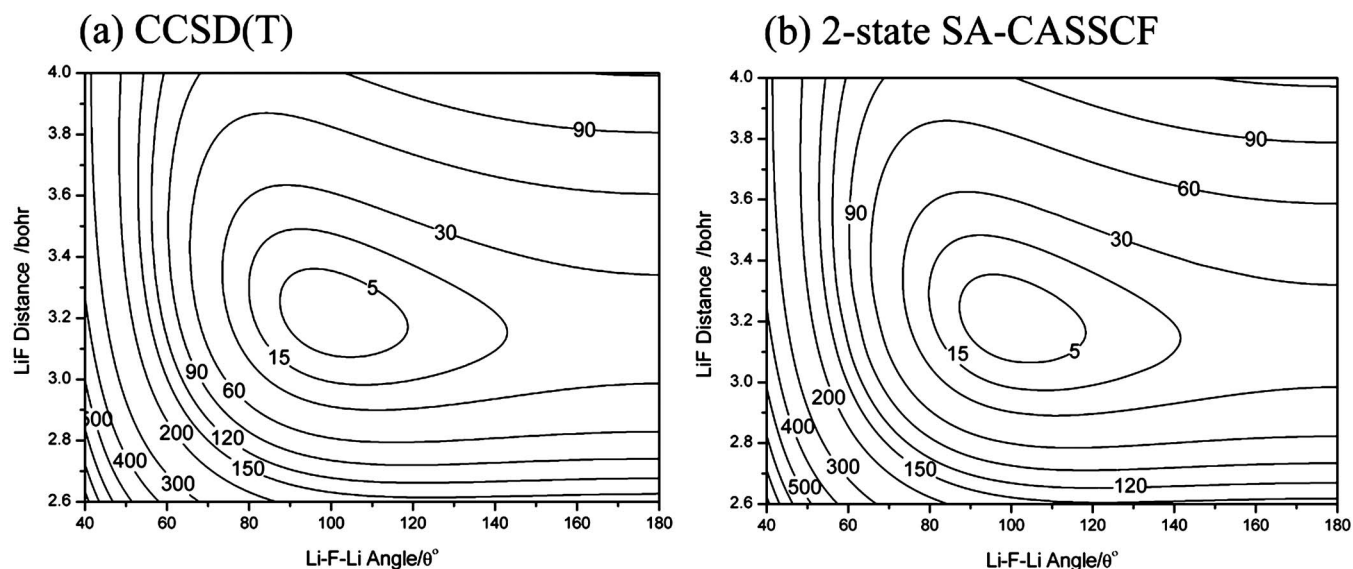


FIG. 1. (a) CCSD(t) potential of the global minimum in the X^2A_1 potential of the Li_2F molecule with the geometry held at C_{2v} in all calculations. (b) Equivalent surface calculated using a two state SA-CASSCF calculation. Energies are in kJ mol^{-1} with zero energy corresponding to the global minimum for the LiFLi molecule in the X^2A_1 state.

has also been identified in $\text{Li}+\text{FLi}$ by Sengupta and Chandra⁶ using coupled cluster calculations. The first excited $^2A'$ surface was predicted as having a minimum in the linear KCINa geometry though the potential was very flat between 180° and 120° . It is important to note that these potentials were based on just 120 calculated points, each involving just 4000 CSFs.

One drawback of the most recent theoretical work is that it has concentrated on the use of single reference quantum methods such as MP2, CCSD(T), etc. The switch in bonding, from covalent (neutral $\text{Li}+\text{LiF}$ fragments) to ionic (at the global minimum), means that the problem is correctly treated by using multireference techniques such as Complete Active Space Self-Consistent Field (CASSCF) and MultiReference CI (MRCI). Gao *et al.* have conducted a CASSCF and MRCI study¹⁶ but have performed the calculation with seven electrons in ten orbitals, a $\text{CAS}(7,10)$ calculation in their nomenclature, whereas a full valence calculation would be $\text{CAS}(9,12)$. In this paper, the lowest three electronic states of Li_2F are investigated by *ab initio* quantum chemistry using all the valence electrons and orbitals. The CASSCF method is used to clarify the origin of the ionic-covalent interaction and in particular the geometric dependence of any curve crossings. Nonadiabatic effects, in particular the crossing of covalent and ionic potentials, are important in the diatomic alkali halide species^{17,18} though there is an absence of detailed *ab initio* work on the corresponding triatomic systems. Unfortunately, the CASSCF method, though relatively inexpensive and multireference in nature, does not capture the dynamic electron correlation, though in this system these effects might be expected to be relatively insignificant. To explore this more fully, CCSD(T) (single reference) and MRCI (multireference) calculations are presented to test the validity of the CASSCF method in such a system. Comparison will be made between the results here and earlier treatments, particularly the pseudopotential work.

II. AB INITIO CALCULATIONS

Calculations were performed at the CCSD(T), CASSCF, and MRCI(Q) (MRCI with Davidson correction) levels using either GAUSSIAN 98 (Ref. 19) and GAUSSIAN 03 (Ref. 20) or PC GAMESS/FIREFLY (Ref. 21) running on a mixed cluster of Core 2 Duo (E6550 2.33, E6600 2.4, E6750 2.66, and E8200 2.66 GHz) and Quad (Q6700 2.66 GHz) PCs all with 2Gbyte of RAM. As this paper is concerned with two different molecular geometries of Li_2F , two different coordinate systems are adopted. The first is a special case of Radau coordinates used to describe the LiFLi hypermetalated molecular system. The second is the three-atom Jacobi coordinates and describes the $\text{LiF}+\text{Li}$ exchange reaction. In all calculations the augmented correlation consistent triple zeta (aug-cc-pVTZ or AVTZ) basis set for both fluorine^{22,23} and lithium²⁴ atoms (denoted here as an AVTZ/AVTZ calculation) is adopted.

CCSD(T) and CASSCF calculations of the LiFLi molecule about its minimum geometry were conducted and compared with the results of Koput. This is to validate the CASSCF method as an accurate description of the ground potential surface. One significant distinction, however, is that the majority of the calculations presented (Fig. 1) in this work involve the valence electrons only, with the $1s$ orbitals on the atoms frozen. One advantage of the CASSCF method is the ability to calculate multiple potential surfaces of identical symmetry and therefore reveal avoided crossings between surfaces, though the resulting state-averaged CASSCF (SA-CASSCF) wave functions are inevitably less accurate than a single state CASSCF or CCSD(T) wave function. For the purposes of determining the influence of electron correlation on the ground state surface the SA-CASSCF calculation was performed over two states (two-state SA-CASSCF) and the ground state surface (Fig. 1) compared with the CCSD(T) potential.

The second group of surfaces, for the $\text{LiF}+\text{Li}$ exchange reaction, used additional SA-CASSCF calculations over the

TABLE I. The equilibrium geometries for the ground and excited electronic states of the Li₂F molecule calculated at the CCSD(T), three-state SA-CASSCF and MRCI(Q) levels with the AVTZ basis set for both atoms. The angle measured is the interior angle in the LiFLi system formed from the two LiF bonds: this angle is not defined in the LiLi'F geometry (the Li–Li separation is 3.3524 Å). Zero energy is defined by the fragments LiF and Li in their ground states (calculated by each method in turn) with the LiF bond length set at the energy minimum (calculated by CASSCF as 2.97a₀) and the fragments separated by 30a₀. The MRCI(Q) calculations used the same geometry that was optimized at the three-state SA-CASSCF level and therefore is not representative of the exact global MRCI(Q) minima.

Method	State	$r(\text{Li}'\text{F})/\text{\AA}$	Θ (°)	Energy/ E_h	Relative energy/kJ mol ⁻¹
HF	X^2A_1	1.669	101.3	-114.469 584 8	-138.41
CCSD(T)	X^2A_1	1.697	100.3	-114.763 191 10	-144.63
CASSCF	X^2A_1	1.696	99.46	-114.635 566 83	-139.78
	$A^2\Sigma_u^+$	1.666	180	-114.610 573 45	-76.56
	$B^2\Pi_g$	1.662	180	-114.575 117 31	15.80
	$X^2\Sigma^+(\text{LiLi}'\text{F})$	1.597	N/A	-114.608 062 98	-17.59
MRCI(Q)	X^2A_1	1.696	99.46	-114.766 752 91	-142.41
	$A^2\Sigma_u^+$	1.666	180	-114.745 902 76	-87.66
	$B^2\Pi_g$	1.662	180	-114.702 807 80	6.93
	$X^2\Sigma^+(\text{LiLi}'\text{F})$	1.597	N/A	-114.719 822 44	-20.23

lowest three states of A' symmetry (valence electrons only). A potential energy surface was constructed from over 600 CASSCF points. In addition, at the two linear configurations (0°, 180°) MRCI(Q) points for the lowest two $^2\Sigma^+$ states were computed based on a two-state SA-CASSCF wave functions and calculated to assess the effects of dynamic electron correlation (or lack of) on the interacting potentials. MRCI(Q) calculations were also performed on the $^2\Pi$ state based on a single CASSCF wave function. With the MRCI(Q) calculations the lowest three orbitals were closed while the remaining 162 were opened allowing for single and double excitations out of the valence reference space. As a result the electronic wave function was generated from over 19×10^6 CSFs, creating a rather large and computationally expensive calculation. The potentials were fitted at long range so that they corresponded with the asymptotic limit thus enabling both the $^2\Sigma^+$ and $^2\Pi$ states to be compared. Details of all three potentials calculated are presented in Table I.

III. RESULTS AND DISCUSSION

A. LiFLi molecule

In Fig. 1(a), the calculated CCSD(T) potential in C_{2v} symmetry around the global minimum is presented. This dictates the bending motion through the LiFLi linear geometry and clearly shows the unstable linear $D_{\infty h}$ isomer observed elsewhere as a local maximum (saddle point) in the bending potential. The minimum geometry here calculated with the AVTZ/AVTZ basis set (100.30° and 1.697 Å) is similar to that calculated¹ by Koput with the larger V5Z/AV5Z basis set (101.2° and 1.686 Å). Indeed the resulting Li–F–Li angle lies in between that of the VTZ/AVTZ and VQZ/AVQZ calculations reported by Koput. Overall a trend emerges that triple zeta basis sets underestimate the bond angle while overestimating the bond length. The results obtained here are also consistent with the DFT, MP2, and CCSD(T) calculations by Ochsenfeld and Ahlrichs²⁵ and Sengupta *et al.*⁶ The three harmonic vibrational frequencies were calculated at the

HF (241.397, 677.22, and 711 cm⁻¹), single state CASSCF (236.90, 649.81, and 678.54 cm⁻¹), and CCSD(T) (248.02, 637.51, and 673.49 cm⁻¹) levels using the same basis set, showing the effect of increased electron correlation is to reduce the vibrational frequencies of the highest energy modes. The saddle points are located in the $D_{\infty h}$ linear geometry at 1.667 Å [CCSD(T) calculation] and 1.662 Å (two-state SA-CASSCF) with barrier heights of 1775 and 1846 cm⁻¹, respectively. The additional stabilization of the transition state thanks to dynamic electron correlation lowers the barrier height in the CCSD(T) result.

Koput also calculated the minimum at the complete basis set (CBS) limit and furthermore included relativistic and core-valence effects to determine the equilibrium geometry as 101.00° and 1.671 Å. The importance of electron correlation among the core electrons was highlighted in that work, with the major contribution being a reduction in the Li–F bond length of the order -0.018 Å. However, Iron *et al.*²⁶ have shown that in general the core-valence correlation is small for lithium based compounds compared to the other alkali metals. To assess the influence of core-valence effects, calculations were performed on the ground state using the CASSCF, CCSD(T), and MRCI methods with the aug-pCVTZ basis set²⁷ developed by Woon and Dunning. The dissociation energy of the molecule calculated by the three methods is compared with previous studies in Table II. When the calculation includes only the valence electrons, the changes in geometries and energies are less than 1%. However, when the core electrons are included, the changes are more significant: at the CCSD(T) level, the changes are -0.012 Å, +0.21° and +2.02 kJ mol⁻¹. These changes are still, however, within “chemical accuracy” and therefore the smaller AVTZ basis set is used in our subsequent calculations. Further support was provided by calculations of the SA-CASSCF equilibrium geometry for all three states using the aug-pCVTZ basis set and an active space including either the valence electrons alone or all the electrons. Comparing the two basis sets, the X -state geometry with a valence (full)

TABLE II. Dissociation energies and global minima of the Li_2F molecule calculated in a variety of *ab initio* studies. The value taken from Koput's work is that quoted as his most accurate, while the only other MRCI(Q) calculation was performed by Chen and was not at the global minimum.

Authors	Method/basis set	$r(\text{LiF})/\text{\AA}$	Θ ($^\circ$)	$D_e/\text{kJ mol}^{-1}$
This work	CCSD(T)/AVTZ	1.697	100.30	144.63
This work	MRCI(Q)/AVTZ ^a	1.697	100.30	146.05
This work	CCSD(T)/ACVTZ (valence only)	1.693	100.39	144.54
This work	CCSD(T)/ACVTZ (all electrons)	1.681	100.18	146.56
This work	MRCI(Q)/ACVTZ	1.693	100.39	147.96
Koput ^b	CCSD(T)/CBS ^c	1.671	101.00	147.62
Chen ^d	MRCI(Q)/AVTZ ^e	1.693	100	142.59
Rehm ^f	MP2/6-31+G*	1.676	107.1	143.51
Sengupta ^g	MP2/6-311++G**	1.697	101.5	142.0
Kudo ^h	DFT (B3LYP)/6-311+G(d)	1.682	110.0	147.4
Ahlrichs ⁱ	CCSD(T) ^j	1.667	101.8	145.4

^aAbsolute energy $-114.768\,139\,43$ hartree.

^bReference 1.

^cCBS limit based on cc-pVnZ ($n=3-5$) basis set calculations and includes an additional core orbital correction term estimated at the cc-pCVnZ ($n=3$ and 4) level, higher-order valence-electron correlation contributions and scalar relativistic effects.

^dReference 28.

^eCalculation performed with MOLPRO (Ref. 29).

^fReference 5.

^gReference 6.

^hReference 12.

ⁱReference 25.

^jCustom basis set Li ($10s, 5p, 2d$)/[$6s, 5p, 2d$] and F ($10s, 7p, 3d, 2f$)/[$6s, 5p, 3d, 2f$].

electron calculation changed by -0.08° ($+0.28^\circ$) and -0.001 \AA (-0.004 \AA) compared to the computationally less intensive AVTZ basis set. For the excited states, the $A\ ^2\Sigma_u^+$ minimum shrinks by 0.008 \AA (0.010 \AA) and $B\ ^2\Pi_g$ by 0.002 \AA (0.003 \AA). Clearly, the accuracy of the AVTZ, valence electron only, calculations is acceptable.

The CCSD(T) potential surface presented here was calculated in less than three days on a pair of Core 2 Duo computers, a comparable time to that for a single (three-state) MRCI(Q) point in C_s symmetry. The corresponding ground state potential from a two-state SA-CASSCF calculation with the same basis set is presented in Fig. 1(b) and is strikingly similar to the CCSD(T) potential, demonstrating that the SA-CASSCF results are of comparable quality. Indeed the only noticeable difference is that the CASSCF potential appears to be slightly “steeper.” The global minimum is, however, calculated to be $\sim 1^\circ$ tighter than the CCSD(T) result, though the bond length is within 0.1 p.m. The SA-CASSCF and CCSD(T) calculations took a comparable computation time, but of course the former allowed two potentials to be computed simultaneously. The similarity between the two calculations reveals that the dynamic electron correlation, although still important for absolute energies, only adds a small contribution to the shape and depth of the ground state potential close to the global minimum.

The MRCI(Q) calculations in Table I are based on the geometries found using an optimization routine at the CASSCF level. However, the presence of dynamic electron correlation in the ground state, as exemplified by the CCSD(T) result, alters the minimum geometry in the ground state. It is reasonable to suppose that the geometry found by CCSD(T) is more accurate than the CASSCF result. There-

fore, the MRCI(Q) calculation was repeated at the CCSD(T) geometry (Table II) and the calculated MRCI(Q) bond dissociation energy is clearly an improvement on the three-state SA-CASSCF based geometry in Table I. The value calculated here with the CASSCF method is 6.27 kJ mol^{-1} higher in energy than that calculated by MRCI(Q) which is 1.42 kJ mol^{-1} lower than the corresponding CCSD(T) value. The values for the dissociation energy calculated by both the coupled cluster and configuration interaction methods are in good agreement with previous work using similar sized basis sets. Ignoring the previous calculations by Rehm *et al.*⁵ and Haketa *et al.*¹² because the bond angle seems rather large in their work and the calculation by Chen²⁸ which is not at the equilibrium geometry, the average theoretical dissociation energy D_e is $146.11 \pm 1.36(\text{std})\text{ kJ mol}^{-1}$.

B. Li+LiF exchange

To explore the ground state potential in further detail, a three-state SA-CASSCF calculation of the lowest $^2A'$ potentials was performed in C_s symmetry using Jacobi coordinates to describe the Li+LiF system. This encompassed a larger range of molecular geometries than the CCSD(T) calculation and should more accurately describe the exchange reaction Li+LiF. Such potentials would be useful for scattering calculations and for modeling the cooling of LiF molecules by ultracold Li atoms (buffer gas cooling). The polar plot in Fig. 2 depicts the Li+LiF potential energy surfaces for the ground $X\ ^2A'$ and first excited $A\ ^2A'$ states with the LiF diatomic bond length held at $3a_0$, close to the equilibrium bond distance calculated by CASSCF ($2.99a_0$). These calculations reveal the presence of a second minimum on the $X\ ^2A'$ poten-

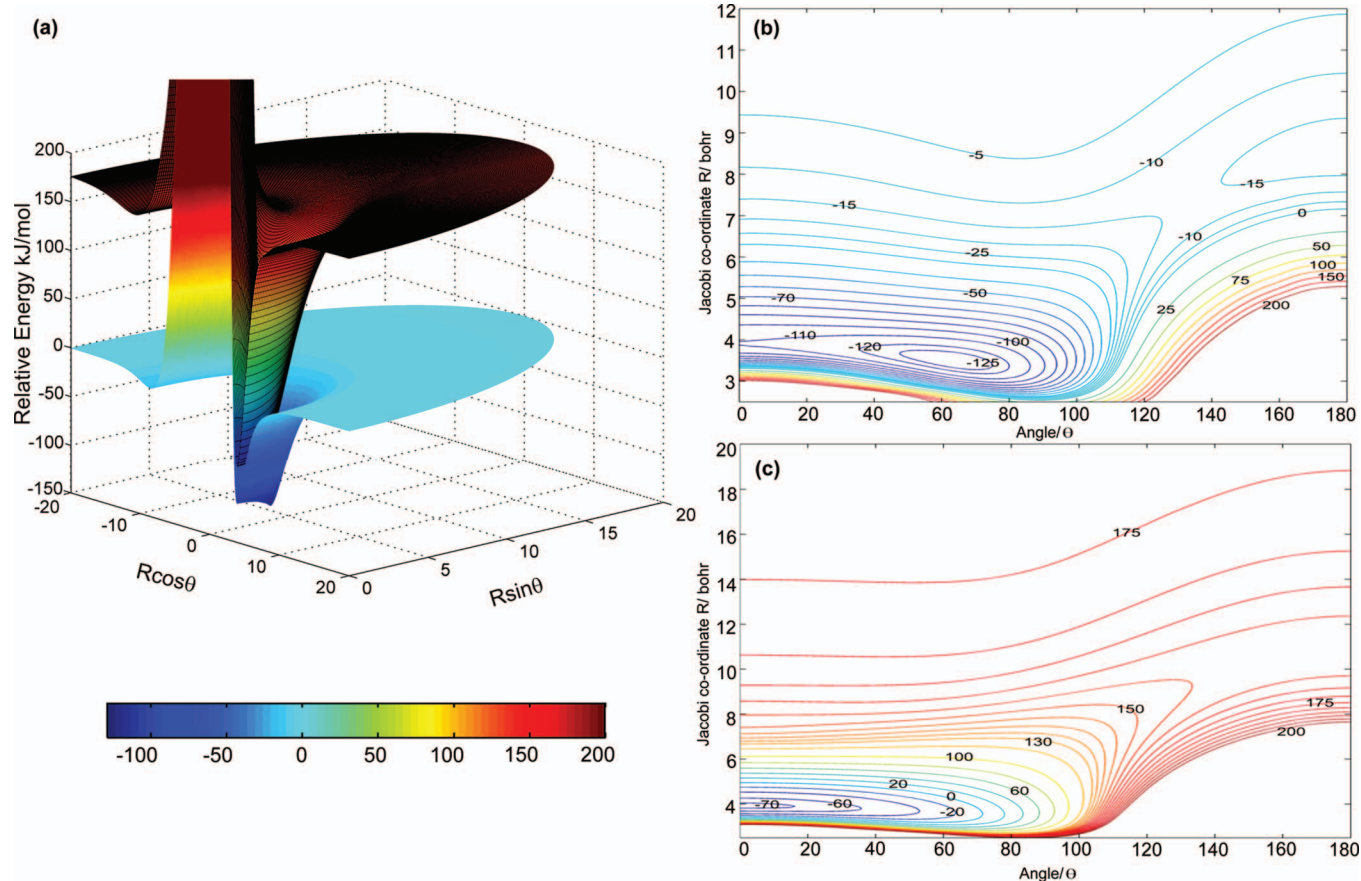


FIG. 2. (a) A polar (R, θ) plot of the lowest two $^2A'$ states with the LiF bond length fixed at $3a_0$. The surfaces are based on three state SA-CASSCF calculations using the AVTZ/AVTZ basis set for all atoms. The energy scale is in kJ mol^{-1} with zero energy corresponding to the lowest LiF+Li asymptote. The calculated energy separation between the two asymptotes is $14\,846\text{ cm}^{-1}$ ($177.60\text{ kJ mol}^{-1}$), while the experimental value for the $\text{Li}(^2S) \rightarrow \text{Li}(^2P)$ transition is $14\,903\text{ cm}^{-1}$ ($178.28\text{ kJ mol}^{-1}$). $R\cos\theta$ and $R\sin\theta$ are in atomic units. (b) Contour plot of the angular dependence of the ground $X\ ^2A'$ state, while (c) is the same but for the $A\ ^2A'$ state.

tial corresponding to the linear LiLiF geometry. This minimum is considerably shallower than the global minimum calculated earlier with a depth of just 17.59 kJ mol^{-1} , in agreement with the result⁴ from Pearson *et al.*, and about half the pseudopotential value³ of Struve. The ground state surface in Fig. 2 has a barrier, corresponding to the molecular rearrangement from the $X\ ^2\Sigma^+$ ($\text{LiLi}'\text{F}$) configuration to the $X\ ^2A_1$ configuration, of 2.6 kJ mol^{-1} . Such a potential may support a ground vibrational state of the $\text{LiLi}'\text{F}$ molecule, though in this instance it is unlikely as the zero point energy for $X\ ^2\Sigma^+$ ($\text{LiLi}'\text{F}$), calculated from the harmonic vibrational frequencies, is 6 kJ mol^{-1} , greater than the angular barrier and hence the linear LiLiF isomer cannot be isolated.

The global minimum in the $X\ ^2A'$ state sits some 140 kJ mol^{-1} below the LiF+Li asymptote and the linear saddle point is clearly identified. The SA-CASSCF calculations demonstrate that the interaction between the Li atom and the LiF molecule is attractive on both surfaces for all lithium atom approaches. There is no evidence of a repulsive interaction as suggested by Chandra and co-workers⁶ and the SA-CASSCF ground state potential is broadly similar to the semiempirical potential of Roach and Child² except that the $D_{\infty h}$ geometry is lower in energy than $C_{\infty v}$ for the Li_2F system, in agreement with Haketa *et al.*¹² It has been postulated² that the dissociation energy of M_2X molecule will be simi-

lar to the dissociation energy of the M_2^+ cation. The calculated dissociation energy [MRCI(Q)] is $12\,209\text{ cm}^{-1}$ ($146.05\text{ kJ mol}^{-1}$), rather higher than the Li_2^+ cation which is calculated³⁰ as $10\,425\text{ cm}^{-1}$ ($124.71\text{ kJ mol}^{-1}$). The value here is almost identical to that found by Pearson *et al.*⁴ and some 50% deeper than the pseudopotential calculation. Clearly, an isolated Li_2F radical in its ground state is very stable to fragmentation and its experimental fragility must be a consequence of its chemical reactivity. Figure 2 also emphasizes that the energy range studied by Koput¹ is just a small part of the deep ground state potential well. Inspection of the electronic wave function indicates that this minimum is ionic in nature and Figs. 3 and 4 reveal that the lowest three $^2A'$ states are the result of extensive avoided crossings between ionic and covalent potentials.

C. Excited electronic states

Figures 2 and 3 illustrate how the bottom of the $A\ ^2A'$ potential lies within 64 kJ mol^{-1} of the global $X\ ^2A'$ minimum and considerably below the Li+LiF asymptote. At long internuclear distances, the $X\ ^2A'$ state is covalent and is bound thanks to a dipole-atom interaction potential, clearly visible at the larger Jacobi angles. As the angle decreases (the Li approaches the fluorine side of the diatomic) the co-

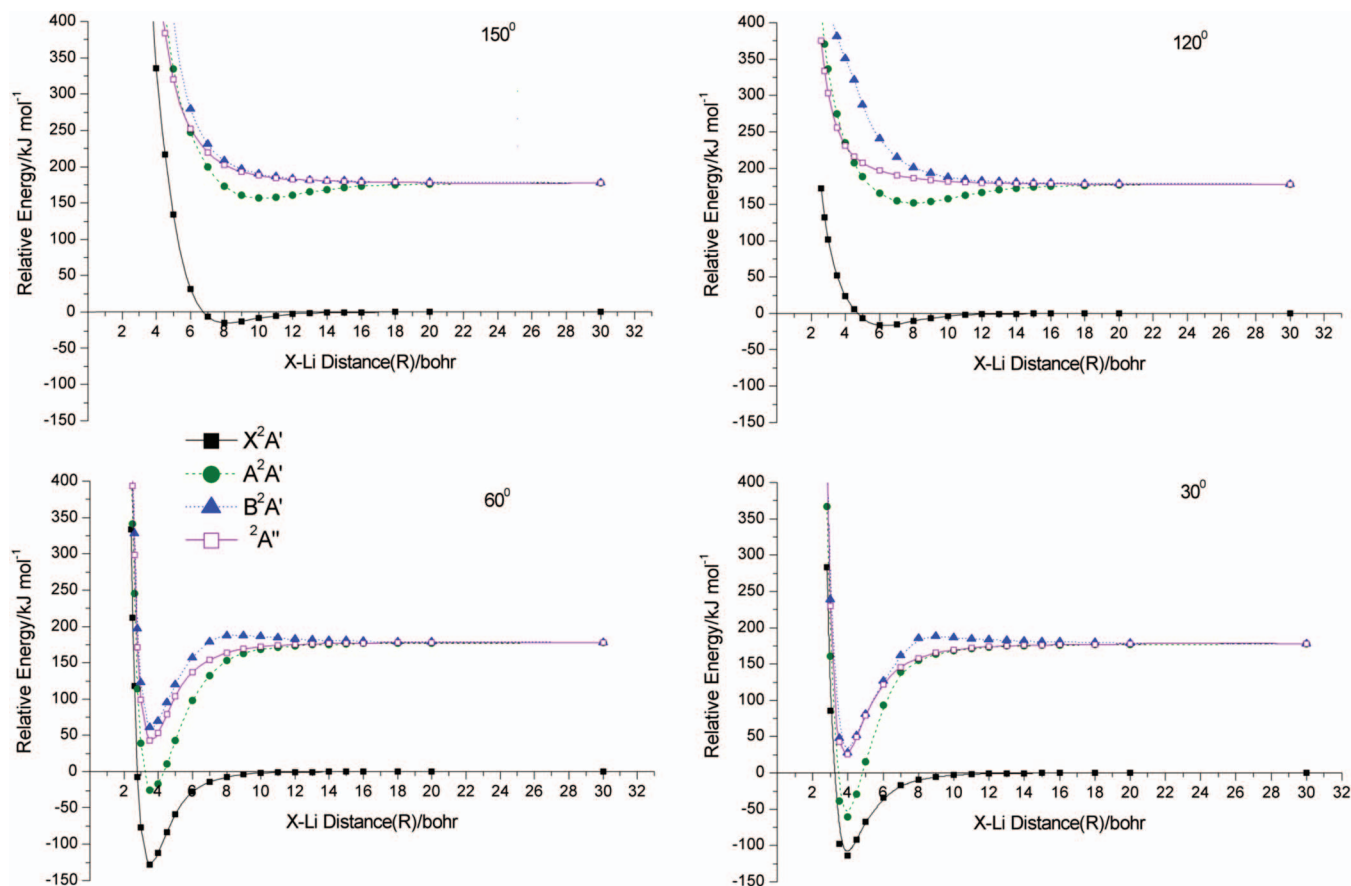


FIG. 3. SA-CASSCF calculations of the lowest three ${}^2A'$ states (solid dots) and ${}^2A''$ state (open dots) in Li_2F at various angles. 0° is set at the colinear $\text{LiF} + \text{Li}$ reaction, while 180° is the colinear $\text{Li} + \text{LiF}$ reaction and the r coordinate set at $3a_0$. Lithium distance measured from LiF center of mass (Jacobi R coordinate) and energies are in kJ mol^{-1} . Zero energy corresponds to the fragments LiF and Li in their ground states.

valent surface is crossed by an ionic state following electron transfer from the Li atom to the LiF diatomic. Consequently, the $A {}^2A'$ state is formed from the lowest covalent surface at short range and from the ionic potential beyond this inner crossing point. Furthermore, the minimum of the $A {}^2A'$ is actually a linear $A {}^2\Sigma_u^+$ state and not the triangular configuration suggested by Struve.

Three further observations about the lowest two ${}^2A'$ surfaces should be made. First, care must be taken when comparing the ionic-covalent interaction seen here to a classic harpoon interaction. Comparison of the potentials at different Jacobi angles θ (Fig. 3) illustrates that the ionic-covalent interaction changes with the angle of the Li atom relative to the LiF molecule. Therefore, in this case there is no such thing as a “harpoon radius.” Rather it may be thought of as a harpoon arc or cone as the electron transfer process clearly demonstrates a significant stereodynamic character on the three lowest potentials. The ionic potential does not cross the covalent state in the LiLiF geometry and thus the minimum of the ionic surface lies above the $\text{Li} + \text{LiF}$ asymptote. The ionic potential curve cannot be simulated by a simple Rittner potential,³¹ unlike other harpoon type mechanisms. On the ground state surface the avoided crossing takes place at around $4.5a_0$ in the LiFLi arrangement, a result in broad agreement with Morokuma.¹⁵ Evidence for a similar crossing can be seen at $\sim 7a_0$ in the $A {}^2\Sigma_u^+$ state.

Second, the presence of the minimum on the second ${}^2A'$ state below the $\text{Li} + \text{LiF}$ asymptote means that collisions between these species involve both the $X {}^2A'$ and $A {}^2A'$ surfaces and consequently nonadiabatic effects cannot be ignored. The fact that the excited state lies deep within the ground state minimum is another new result here, as Struve places the minimum of the $A {}^2A'$ excited state of $\text{Na} + \text{NaCl}$ well above the ground asymptote (by at least 40 kJ mol^{-1}). Third, the low lying $A {}^2A'$ state means that the vibrational and rotational levels of the ground $X {}^2A'$ state will suffer a great deal of perturbation by the interloping state. However, the calculations of Koput dealt with the energy region below the ground state saddle point and hence were not affected by the presence of the low lying $A {}^2A'$ potential minimum. Calculation of the lowest ${}^2A''$ state (Fig. 3) effectively allows the geometric behavior of the $B {}^2\Pi$ state to be followed and facilitates the identification of the $A {}^2\Sigma^+$ and $B {}^2\Pi$ components of the $A {}^2A'$ potential. Initially the $A {}^2A'$ potential at 0° (180°) follows the $B {}^2\Pi$ potential well but crosses to the $A {}^2\Sigma^+$ state, forming an avoided crossing at nonlinear geometries. The three state SA-CASSCF calculation of the $B {}^2A'$ state reveals it is also the result of such an interaction, the ionic state just visible as a kink in the repulsive covalent state [correlating to $\text{Li}({}^2P) + \text{LiF}$] at $\theta = 120^\circ$. The minimum of the $B {}^2A'$ state is ionic with $D_{\infty h}$ symmetry and lies within

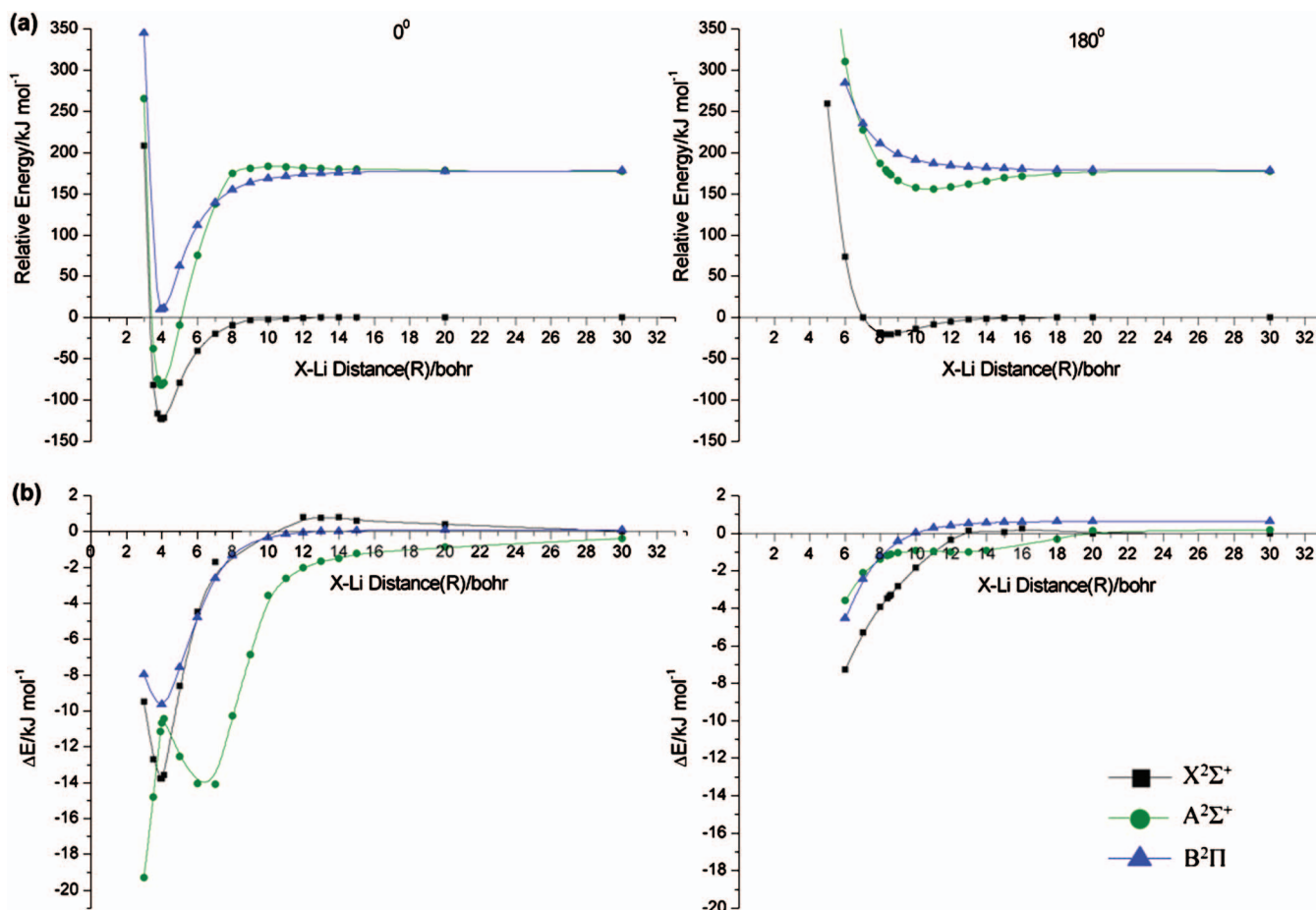


FIG. 4. (a) MRCI(Q) (solid dots and lines) calculations of the lowest three states in Li₂F, in the two colinear arrangements with 0° corresponding to the LiFLi and 180° the LiLiF conformation. The r coordinate is set at $3a_0$ and the energies are in kJ mol⁻¹. Zero energy corresponds to the fragments LiF and Li in their ground states. (b) The difference in relative energy between SA-CASSCF and MRCI(Q) calculations as a function of lithium atom distance R (Jacobi coordinates).

15 kJ mol⁻¹ of the ground state asymptote. At long-range it possesses a small barrier for Li(²P)+LiF collisions at small values of θ .

D. Dynamic electron correlation

MRCI(Q) calculations were performed at the two colinear geometries on the potential surfaces in order to explore further any possible effects due to dynamical electron correlation on both the ground and excited surfaces. Again, the diatomic alkali halides have been a popular system for studying the effects of dynamic electron correlation effects, especially LiF.^{32,33} Each CI point in C_{2v} ($C_{\infty v}$) symmetry took around 30 h of CPU time and the Davidson correction was included in the calculations. Figure 4(a) shows the lowest three states calculated at the MRCI(Q) levels in the linear geometries LiLiF and LiFLi($2x^2\Sigma^+$ and $1x^2\Pi$). The MRCI(Q) and SA-CASSCF potentials are almost identical. In Fig. 4(b) the differences in relative energy between MRCI(Q) and SA-CASSCF points are plotted for the two linear geometries. It clearly shows that the difference in energy between the methods is greater for the LiF+Li approach geometry than for Li+LiF. This result is rather counterintuitive as one would expect that dynamic electron correlation would be greater in the LiLiF than in the LiFLi arrangement,

due to the nonionic nature of the bonding. The SA-CASSCF barrier on the $A^2\Sigma^+$ state (green line) at zero degrees is 9.91 kJ mol⁻¹, though it is markedly reduced in height by including the extra electron correlation (to 5.43 kJ mol⁻¹) in the MRCI(Q) calculation. The most significant differences, however, are situated in the repulsive wall of the potential where the rate of change of energy with bond distance is the greatest. The similarity between the MRCI(Q), CCSD(T), and SA-CASSCF potentials is consistent with the remarkably successful semiempirical potentials that were calculated using a model of a single valence electron moving in a potential field² generated by the metal ion cores and the F⁻ anion.

The covalent component of the X^2A' surface is also attractive and the minimum is due to a long-range dipole-induced dipole interaction first discovered in the K+RbCl reactive scattering experiment of Miller *et al.*,³⁴ which was also the first to demonstrate the formation of a long lived collision complex in an exchange reaction. The present calculations confirm that the long-range potential is indeed of a dipole-induced dipole type as the covalent-ionic crossing takes place at a relatively short range. The repulsive wall of all three potentials are pushed to longer distances in the LiLiF geometry because the van der Waals radius³⁵ of Li is greater than F and the separation is determined from the LiF

center of mass (which is not at the center of the LiF bond). Cao *et al.*¹⁶ have reported a X^2A_1 global minimum, a first excited state that is linear¹⁶ with $^2\Sigma_g^+$ symmetry (but an imaginary bending frequency) and a “stable” excited state of $^2\Sigma_u^+$ symmetry. However, the results presented here show that the “unstable” $^2\Sigma_g^+$ state is in fact the saddle point on the ground X^2A' global surface, which does indeed have symmetry 2A_1 at its minimum, and that the lowest excited state is $^2\Sigma_u^+$ at its equilibrium geometry.

The MRCI(Q) calculation reduces the energy of the $B^2\Pi$ state minimum so that it now lies within 7 kJ mol⁻¹ of the ground state asymptote. As the zero point energy of LiF is 455 cm⁻¹ (5.4 kJ mol⁻¹), this suggests that even an ultracold collision with a ground rovibrational LiF molecule could involve as many as three potential energy surfaces (making the reasonable assumption that the well will deepen at the CBS limit). This is a rather unexpected situation as the Li(²S)+LiF(¹Σ⁺) asymptote correlates with just a single (nondegenerate) potential energy surface and there is no reaction barrier. As the additional electronic states are bound, scattering resonances will feature prominently in the collision dynamics. Following the argument of Roach and Child, the effect of these nonadiabatic transitions will be to increase the reactive cross sections relative to those for inelastic scattering, a phenomenon first observed³⁶ in the KBr+Na system by Moulton and Herschbach. In that particular experiment, the reactive cross section was ten times that of the nonreactive, a result that could have significant consequences for attempts to sympathetically cool alkali halides with ultracold alkali atoms.

It has been previously noted³⁷ that electron correlation effects do not have a strong effect on the F+Li₂ surface (as well as H+Li₂). The present results indicate that this is not entirely true over the whole potential and it is clearly significant for the A^2A' excited state potential about its potential minimum and for describing the barrier on the B^2A' state. However, large parts of the ground state surface are indeed modeled well by the SA-CASSCF method. For ultracold collisions, it is possible that any differences are essentially irrelevant because of the long de Broglie wavelengths of the reagents. A comparison of quantum scattering calculations at ultralow energies on SA-CASSCF and MRCI(Q) surfaces would be instructive.

IV. CONCLUSION

High-level *ab initio* calculations on the Li₂F molecule have revealed the presence of two minima on the ground surface, one corresponding to an ionic molecule and the second, shallower well to a dipole-induced dipole interaction. At extended lithium distances, the ionic attraction is between Li⁺ and the LiF anion. The global minimum for X^2A' calculated here is consistent with the recent results by Koput and others but the relative well depths calculated are at variance with semiempirical potentials for similar alkali+alkali halide systems. The first two excited states possess very deep potential wells in the $D_{\infty h}$ geometry that will influence both the rovibrational levels of the ground state and the scattering dynamics, even at ultracold temperatures. It was also found

that dynamic electron correlation effects were relatively small in this system, a result that is consistent with previous work on lithium containing compounds. Consequently, SA-CASSCF calculations prove to be surprisingly accurate, even for the electronically excited states.

ACKNOWLEDGMENTS

The authors would like to thank Carolyn Devlin and Ruiping Chen for their help with this publication. K.W.A.W. and D.E.R. would like to thank DEL for studentships.

- ¹J. Koput, *J. Chem. Phys.* **129**, 154306 (2008).
- ²A. C. Roach and M. S. Child, *Mol. Phys.* **14**, 1 (1968).
- ³W. S. Struve, *Mol. Phys.* **25**, 777 (1973).
- ⁴P. K. Pearson, W. J. Hunt, C. F. Bender, and H. F. Schaefer, *J. Chem. Phys.* **58**, 5358 (1973).
- ⁵E. Rehm, A. L. Boldyrev, and P. v. R. Schleyer, *Inorg. Chem.* **31**, 4834 (1992).
- ⁶D. Sengupta and A. K. Chandra, *J. Mol. Struct.: THEOCHEM* **492**, 29 (1999).
- ⁷S. R. Velickovic, L. T. Petkovska, and A. A. Peric-Grujic, *Chem. Phys. Lett.* **448**, 151 (2007).
- ⁸M. J. Polce and C. Wesdemiotis, *Int. J. Mass Spectrom.* **182/183**, 45 (1999).
- ⁹M. Veljković, O. Nešković, M. Miletic, and K. F. Zmbov, *Rapid Commun. Mass Spectrom.* **10**, 619 (1996).
- ¹⁰K. Yokoyama, N. Haketa, H. Tanaka, K. Furukawa, and H. Kudo, *Chem. Phys. Lett.* **330**, 339 (2000).
- ¹¹O. M. Neskovic, M. V. Veljkovic, S. R. Velickovic, L. T. Petkovska, and A. A. Peric-Grujic, *Rapid Commun. Mass Spectrom.* **17**, 212 (2003).
- ¹²N. Haketa, K. Yokoyama, H. Tanaka, and H. Kudo, *J. Mol. Struct.: THEOCHEM* **577**, 55 (2002).
- ¹³M. Gutowski and J. Simons, *J. Chem. Phys.* **100**, 1308 (1993).
- ¹⁴G. G. Balint-Kurti, Ph.D. thesis, Columbia University, 1969.
- ¹⁵K. Yamashita and K. Morokuma, *J. Phys. Chem.* **92**, 3109 (1988).
- ¹⁶Z. Cao, H. Xian, W. Hu, and Q. Zhang, *Chem. Phys.* **243**, 209 (1999).
- ¹⁷H. J. Werner and W. Meyer, *J. Chem. Phys.* **74**, 5802 (1981).
- ¹⁸P. F. Weck, K. Kirby, and P. C. Stancil, *J. Chem. Phys.* **120**, 4216 (2004).
- ¹⁹M. J. Frisch, G. W. Trucks, H. B. Schlegel *et al.*, GAUSSIAN98, Revision A.1, Gaussian, Inc., Pittsburgh PA, 1998.
- ²⁰M. J. Frisch, G. W. Trucks, H. B. Schlegel *et al.*, GAUSSIAN03, Revision A.1, Gaussian, Inc., Pittsburgh PA, 1998.
- ²¹A. Granovsky, PC GAMESS version 7.0, <http://classic.chem.msu.su/gran/gamess/index.html>.
- ²²T. H. Dunning, Jr., *J. Chem. Phys.* **90**, 1007 (1989).
- ²³R. A. Kendall, T. H. Dunning, Jr., and R. J. Harrison, *J. Chem. Phys.* **96**, 6796 (1992).
- ²⁴D. E. Woon and T. H. Dunning, Jr., EMSL Basis Set Exchange; K. L. Schuchardt, B. T. Didier, T. Elsethagen, L. Sun, V. Gurumoorthi, J. Chase, J. Li, and T. L. Windus, *J. Chem. Inf. Model* **47**, 1045 (2007).
- ²⁵C. Ochsenfeld and R. Ahlrichs, *J. Chem. Phys.* **101**, 5977 (1994).
- ²⁶M. A. Iron, M. Oren, and J. M. L. Martin, *Mol. Phys.* **101**, 1345 (2003).
- ²⁷T. H. Dunning, Jr., *J. Chem. Phys.* **103**, 4572 (1995).
- ²⁸R. Chen, Ph.D. thesis, Queen's University of Belfast, 2005.
- ²⁹MOLPRO, a package of *ab initio* programs designed by H. -J. Werner and P. J. Knowles, Version 2002.6, R. D. Amos, A. Bernhardsson, A. Berning *et al.*
- ³⁰H. Bouzouita, C. Ghanmi, and H. Berriche, *J. Mol. Struct.: THEOCHEM* **777**, 75 (2006).
- ³¹E. S. Rittner, *J. Chem. Phys.* **19**, 1030 (1951).
- ³²C. W. Bauschlicher, Jr. and S. R. Langhoff, *J. Chem. Phys.* **89**, 4246 (1988).
- ³³L. R. Khan, P. Jeffrey Hay, and I. Shavitt, *J. Chem. Phys.* **61**, 3530 (1974).
- ³⁴W. B. Miller, S. A. Safron, and D. R. Herschbach, *Faraday Discuss.* **44**, 108 (1967).
- ³⁵M. Mantina, A. C. Chamberlin, R. Valero, C. J. Cramer, and D. G. Truhlar, *J. Phys. Chem. A* **113**, 5806 (2009).
- ³⁶M. C. Moulton and D. R. Herschbach, *J. Chem. Phys.* **44**, 3010 (1966).
- ³⁷H. F. Schaefer, in *Atom-Molecule Collision Theory*, edited by R. B. Bernstein (Plenum, New York, 1979), Chap. 2, pp. 45–78.